Limnol. Oceanogr., 58(5), 2013, 1747–1760
© 2013, by the Association for the Sciences of Limnology and Oceanography, Inc.
doi:10.4319/lo.2013.58.5.1747

Low nutrient availability reduces high-irradiance–induced viability loss in oceanic phytoplankton

Gemma Kulk,[1,*] Willem H. van de Poll,[2] Ronald J. W. Visser,[1] and Anita G. J. Buma [1]

[1] Department of Ocean Ecosystems, Energy and Sustainability Research Institute Groningen, University of Groningen, Groningen, The Netherlands

[2] Department of Biological Oceanography, Royal Netherlands Institute for Sea Research, Den Burg, The Netherlands

Abstract

In situ viability of oceanic phytoplankton may be relatively low in open oceans. This is assumed to be related to the high-irradiance and low-nutrient conditions typical for oligotrophic regions. However, experimental evidence for this phenomenon was not yet available. In the present study, the importance of nutrient availability in high-irradiance–induced viability loss was therefore studied for three key oceanic phytoplankton species. *Prochlorococcus marinus*, *Ostreococcus* sp., and *Thalassiosira oceanica* were acclimated to two different N : P ratios. Growth, viability, and photophysiology were assessed under nutrient-replete and N- and P-starved conditions. Simultaneously, high-irradiance–induced photoinhibition and viability loss were measured and three inhibitors were used to investigate the underlying physiological mechanisms contributing to viability loss. High-irradiance exposure caused viability loss in *P. marinus* and *Ostreococcus* sp., but not in *T. oceanica*. Low-nutrient availability enhanced survival during high-irradiance exposure, although species-specific differences were observed. The lower sensitivity to high-irradiance intensities at low-nutrient availability was related to conformational changes in photosystem II in *P. marinus*, to enhanced photoprotection by the xanthophyll pigment cycle and alternative electron transport in *Ostreococcus* sp., and to enhanced photoprotection by the xanthophyll pigment cycle in *T. oceanica*. Climate change may lead to enhanced stratification in the open ocean. The resulting increase in the average irradiance intensity phytoplankton experience may promote viability loss in the smallest phytoplankton size fraction. However, this effect may partially be counteracted by the simultaneously expected decrease in nutrient availability.

The phytoplankton community of open oligotrophic oceans is dominated by prokaryotic *Prochlorococcus* spp., *Synechococcus* spp., and eukaryotic pico- and nanophytoplankton (Li 1994; DuRand et al. 2001; Worden et al. 2004). The depth and geographic distribution of these species is often explained by their response to water column conditions (Cavender-Bares et al. 2001; Johnson et al. 2006; Demir-Hilton et al. 2011). For example, high-light–adapted ecotypes of *Prochlorococcus* are adapted to the irradiance and nutrient conditions in the upper mixed layer, with low levels of light-harvesting pigments and a reduced demand in cellular N and P (Moore et al. 1998; Moore and Chisholm 1999; Van Mooy et al. 2009). The contribution of specific phytoplankton species to community primary production may also vary along environmental gradients (Li 1994; DuRand et al. 2001; W. H. Van de Poll et al. 2013). For example, *Prochlorococcus* spp. can contribute 20–40% to the total community production in relatively warm oligotrophic waters, whereas *Synechococcus* spp. and eukaryotic phytoplankton maintain higher production rates when nutrient availability is higher (Vaulot et al. 1995; Worden et al. 2004; W. H. Van de Poll et al. unpubl.). The (dynamic) irradiance and nutrient conditions not only control phytoplankton species distribution and primary production, they have also been related to phytoplankton cell lysis and viability (the fraction of cells with intact membranes; Agustí 2004; Alonso-Laita and Agustí 2006). The viability of oceanic phytoplankton in situ can be relatively low, with viability decreasing up to 50% in both *Prochlorococcus* spp. and *Synechococcus* spp. (Agustí 2004). Moreover, species-specific differences in viability loss have been reported in several oligotrophic regions (Agustí 2004; Sommaruga et al. 2005; Alonso-Laita and Agustí 2006). This can have a major effect on the estimates of primary production and it is therefore important to understand which factors influence viability loss in open oligotrophic oceans.

Similar to the depth and geographic distribution of *Prochlorococcus* spp., *Synechococcus* spp., and eukaryotic pico- and nanophytoplankton, the viability of oceanic phytoplankton species is related to the (dynamic) irradiance conditions encountered in the water column. Phytoplankton irradiance exposure in open oceans can vary by several orders of magnitude due to variations in cloud cover, wind mixing, and stratification (Kirk 2010). In the upper mixed layer, oceanic phytoplankton can experience irradiance intensities that exceed photosynthetic requirements, leading to photoinhibition (loss of functional photosystem II [PSII] reaction centers) and viability loss (Aro et al. 1993; Van de Poll et al. 2006). To avoid photoinhibition and viability loss during high-irradiance exposure, phytoplankton enhance non-photochemical processes, such as the thermal dissipation of excess energy by the xanthophyll pigment cycle, and photochemical processes, such as alternative electron transport and (non-) enzymatic scavenging of reactive oxygen species (Olaizola et al. 1994; Gechev et al. 2006; Raven 2011). Simultaneously, phytoplankton can counteract the effects of

* Corresponding author: g.kulk@rug.nl

photoinhibition by photorepair, a process in which damaged D1 proteins are removed from PSII and replaced by newly synthesized D1 proteins (Aro et al. 1993). Species-specific differences in photoregulation and photorepair have been observed for several oceanic phytoplankton species (Six et al. 2007; Dimier et al. 2009; Kulk et al. 2013), possibly contributing to the distribution of viable cells observed in situ. Moreover, the photoacclimation potential of specific (pico)phytoplankton species may play an important role in the response to (dynamic) irradiance conditions (Kulk et al. 2011).

In addition to irradiance, the depth and geographic distribution of viable *Prochlorococcus*, *Synechococcus*, and eukaryotic pico- and nanophytoplankton cells in open oceans is suggested to be related to nutrient availability (Agustí 2004; Alonso-Laita and Agustí 2006). For example, the viability of *Prochlorococcus* spp. and *Synechococcus* spp. was lower in oligotrophic waters compared with regions influenced by equatorial upwelling in the Central Atlantic Ocean (Agustí 2004). Moreover, nutrient availability has been described to directly affect phytoplankton cell death in cultures (Brussaard et al. 1997; Brussaard and Riegman 1998; Agustí and Sánchez 2002). Nutrient availability is generally low in the open ocean, especially in the upper mixed layer during stratification. Nitrogen (N) is considered the main limiting macronutrient (Graziano et al. 1996; Davey et al. 2008), but on different spatial and temporal time scales, phosphorus (P) may also act as the limiting macronutrient in open oceans (Karl et al. 1997; Cavender-Bares et al. 2001; Wu et al. 2000). In addition to the direct effect of low-nutrient availability on phytoplankton viability, it may have considerable effects on phytoplankton photophysiology and consequently on the response to high-irradiance intensities. Generally, the light-harvesting capacity is reduced during nutrient starvation by a reduction in the cellular chlorophyll *a* (Chl *a*) concentration and quantum yield of PSII, as well as an increase in the relative amount of carotenoids (Geider et al. 1993; Berges and Falkowski 1998; Franklin et al. 2012). However, the absorption of chlorophyll and the absorption cross section of the remaining PSII may increase during nutrient starvation (Geider et al. 1993; Berges et al. 1996), partially counteracting the reduced light-harvesting capacity. Moreover, photochemical energy conversion is affected by a decrease in photosynthetically important proteins such as D1 and Rubisco during N starvation (Geider et al. 1993; Berges and Falkowski 1998; Steglich et al. 2001) and to a lesser extent during P starvation (Geider et al. 1993). It has been suggested that the overall changes in photophysiology during nutrient starvation may lead to an increased susceptibility to high-irradiance intensities in eukaryotic nano- and microphytoplankton (Herzig and Falkowski 1989; Lesser et al. 1994), but decreased sensitivities have also been observed (Van de Poll et al. 2005; Loebl et al. 2010). A direct assessment of the combined effect of high-irradiance exposure and nutrient availability in oceanic pico- and nanophytoplankton is not yet available, despite the relevance for open-ocean water column conditions. It is particularly important to understand oceanic phytoplankton performance given the expected increase in thermal stratification related to climate change, which will enhance the average irradiance intensity phytoplankton experience while simultaneously reducing nutrient availability (Boyd and Doney 2002; Behrenfeld et al. 2006).

In the present study, the importance of nutrient availability in high-irradiance–induced photoinhibition and viability loss was assessed for three key oceanic phytoplankton species. To this end, *Prochlorococcus marinus*, *Ostreococcus* sp., and *Thalassiosira oceanica* were acclimated to two different N : P ratios. Growth, viability, and photophysiology were assessed under nutrient-replete and N- and P-starved conditions by analysis of cell density, membrane permeability, PSII fluorescence, cellular carbon (C), pigmentation, and absorption. Simultaneously, high-irradiance–induced photoinhibition and viability loss were studied under nutrient-replete and -starved conditions. The results are discussed in the context of species-specific differences in photophysiology at low-nutrient availability and are used to unravel the importance of viability loss in the phytoplankton community of open oligotrophic oceans.

Methods

Culture conditions—Cultures were obtained from the Roscoff Culture Collection (RCC) and the National Center for Marine Algae and Microbiota (CCMP). *Ostreococcus* sp. strain RCC410 (ecotype clade B or OII) and *Thalassiosira oceanica* strain CCMP1616 were cultured in K medium based on natural oceanic seawater as described by Keller et al. (1987) without NO_3^-. For *T. oceanica*, silicate was added to the K medium in a final concentration of 50 μmol L^{-1}. *Prochlorococcus marinus* strain CCMP2389 (ecotype MED4) was cultured in a different version of the K medium, with a 10× diluted concentration of trace metals minus copper (K/10-Cu; Chisholm 1992). *P. marinus*, *Ostreococcus* sp., and *T. oceanica* were pre-cultured under two different N : P ratios to establish either nitrogen- (N : P 2) or phosphorus- (N : P 35) starved conditions during the stationary growth phase. To this end, K/10-Cu and K medium were prepared with 100 μmol L^{-1} NH_4^+ and 50 μmol L^{-1} PO_4^{3-} for N : P 2 and 350 μmol L^{-1} NH_4^+ and 10 μmol L^{-1} PO_4^{3-} for N : P 35. Cultures were maintained for several months under these different N : P ratios to ensure acclimation prior to the experiments. Cultures were kept in exponential growth phase (transfer 2 d prior to the stationary growth phase) at 68 μmol photons m^{-2} s^{-1} in a diurnal cycle of 12 : 12 h light : dark (LD) at 20°C and were transferred to the experimental light conditions at least 14 d before the start of the experiment to ensure photoacclimation.

Experimental design—Cultures of *P. marinus*, *Ostreococcus* sp., and *T. oceanica* grown at N : P 2 and N : P 35 were transferred in triplicate to 1 liter glass Erlenmeyer flasks and incubated as batch cultures for a maximum of 14 d at 20°C in an U-shaped lamp setup as described by Van de Poll et al. (2007). Fifty micromoles of photons per square meter per second was provided as a square wave function with a 12 : 12 h LD cycle and irradiance levels were frequently monitored with a Quantum Scalar Laboratory

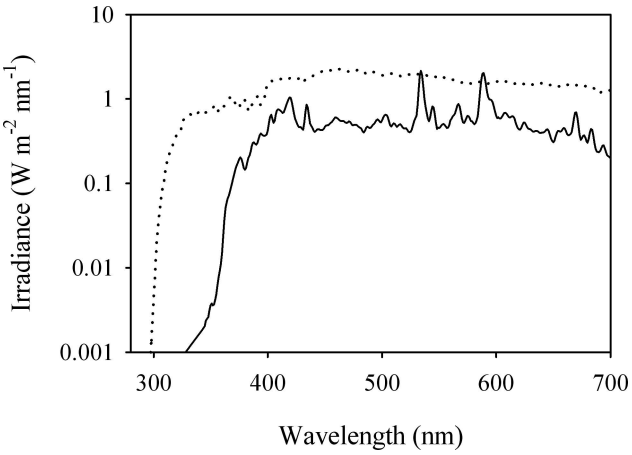

Fig. 1. Spectral irradiance of the high-light treatment (solid line). Corresponding doses were 172 W m^{-2} photosynthetically active radiation (PAR; 400–700 nm) and 8.74 W m^{-2} ultraviolet radiation (UVR; 280–400 nm). A solar spectrum (15:00 h, 02 September 2011, The Netherlands) is given for comparison (dotted line).

100 radiometer (QSL-100, Biosperical Instruments). Samples for the analysis of growth, viability, and the maximum quantum yield of PSII ($F_v : F_m$) were collected daily throughout the experiment. In the mid-exponential growth phase (nutrient-replete samples, at time [t] = 9 d for *P. marinus* and t = 4 d for *Ostreococcus* sp. and *T. oceanica*) and 5 d later in the stationary growth phase (nutrient-starved samples), additional samples were collected for the analysis of non-photochemical quenching (NPQ), elemental composition, pigmentation, and absorption spectra. Nutrient depletion in the stationary growth phase was confirmed by dissolved inorganic phosphate analysis (Murphy and Riley 1962). Simultaneously, viability assays were performed during the exponential and stationary growth phase, in which subsamples were exposed to a high-irradiance treatment to assess survival and photoregulating mechanisms. To this end, four subsamples (20 mL) of each replicate culture were exposed to 500 μmol photons m^{-2} s^{-1} (250 W MHN-TD lamp, Philips) for 4 h. Corresponding irradiance doses were 172 W m^{-2} photosynthetically active radiation (PAR; 400–700 nm) and 8.74 W m^{-2} ultraviolet radiation (UVR; 280–400 nm; Fig. 1). The 10-fold increase in irradiance intensity relates well to water column conditions phytoplankton species encounter in temperate and warm-temperate oceanic regions (also *see* Kulk et al. 2011). For each incubation, the viability of the cells was assessed every 30 min (t = 0, 30, 60, 90, 120, 180, 180, 210, 240 min) by the cell digestion assay (CDA; Agustí and Sánchez 2002) for *P. marinus* and by a SYTOX-Green (Molecular Probes) assay for *Ostreococcus* sp. and *T. oceanica*. Cell densities during the viability assays were ± 5,500,000 cells mL^{-1} in *P. marinus*, ± 2,500,000 cells mL^{-1} in *Ostreococcus* sp., and ± 400,000 cells mL^{-1} in *T. oceanica*. Samples from the stationary growth phase were diluted to these cell densities with nutrient-poor natural seawater, which had no effect on viability for the duration of the measurements (4 h, results not shown). During the viability assay, inhibitors were used to indicate several photoregulating mechanisms, which could be involved in the prevention of photoinhibition and/or viability loss. In addition to a control sample (no inhibitor), subsamples were incubated with Lincomycin (final concentration 0.6 mmol L^{-1}), which inhibits the transcription of chloroplast encoded proteins, such as the D1 reaction center protein (Aro et al. 1993), Propyl gallate (Pgal; final concentration 0.6 mmol L^{-1}), which inhibits a propyl gallate–sensitive oxidase (PTOX) that mediates alternative electron flow to oxygen prior to photosystem I (Bailey et al. 2008), and Dithiothreitol (Dtt; final concentration 0.6 mmol L^{-1}, not for *P. marinus*), which inhibits the de-epoxidation of the xanthophyll pigment cycle (Olaizola et al. 1994). Stock solutions of each inhibitor were freshly prepared in 96% ethanol and culture samples were incubated with each inhibitor under dim light conditions for 10 min prior to the viability assays. In addition to the incubation in high light, control samples were incubated for 4 h in the dark at 20°C. No significant effect of the inhibitors was found on viability during these dark incubations ($p < 0.05$).

Growth measurements—Samples (1 mL) for cell counts were obtained during the exponential and stationary growth phase. Cell concentrations were determined on a Coulter Epics XL-MCL flow cytometer (Beckman Coulter). Growth rates (d^{-1}) of the exponential growth phase were calculated by linear regression of natural log–transformed cell numbers for all replicates (≥ 5 data points). In addition, cell sizes were estimated by calibration of the forward scatter of the flow cytometer (Flow cytometry size calibration Kit F-13838, Molecular Probes).

Viability—Viability of *P. marinus*, *Ostreococcus* sp., and *T. oceanica* was assessed daily and in the exponential and stationary growth phase during high-irradiance exposure. In the eukaryotic species *Ostreococcus* sp. and *T. oceanica*, viability was assessed by a SYTOX-Green assay. SYTOX-Green is a molecular probe that enters cells with a compromised cell membrane, where it binds to double-stranded deoxyribonucleic acid to form a green fluorescent signal (for a review *see* Peperzak and Brussaard 2011). For the assay, a stock solution of SYTOX-Green (1%; Dead Cell Stain, Molecular Probes) was prepared with MilliQ and stored at −20°C. To determine viability, 1 mL culture samples were incubated with SYTOX-Green (final concentration 0.01%) for 30 min in the dark at 20°C. After the incubation, samples were immediately analyzed by flow cytometry (Coulter Epics XL-MCL flow cytometer, Beckman Coulter) and nonviable cells were distinguished from living cells by green fluorescence at 488 nm. Viability (% living cells) was calculated by dividing non–SYTOX-Green-stained cells by the total cell density. Because the prokaryotic species *P. marinus* responds poorly to SYTOX-Green, a CDA as described by Agustí and Sánchez (2002) was used to assess viability in this species. It was previously shown that SYTOX-Green and the CDA yielded similar determinations of viability in numerous phytoplankton species (Agustí and Sánchez 2002; Peperzak and Brussaard 2011). For the CDA, stock solutions of deoxyribonuclease (DNAse) I (800 μg mL^{-1}; Sigma-Aldrich) and Trypsin

(2%; Sigma-Aldrich) were prepared using Hank's balanced salt solution and stored at −20°C. To determine the amount of living cells, 1 mL culture samples were collected and incubated with 150 μL DNAse I solution for 15 min at 37°C. Then, 150 μL Trypsin solution was added and the samples were incubated for another 30 min at 37°C. After incubation, the cell density was immediately analyzed by flow cytometry (Coulter Epics XL-MCL flow cytometer, Beckman Coulter). Total cell density was determined from control samples that were incubated for 45 min at 37°C. Viability (% of living cells) was then calculated by dividing the cell density obtained by the CDA (living cells) by the cell density in the control samples (total cells).

Photosystem II chlorophyll fluorescence characteristics—Photosystem II (PSII) fluorescence analysis were performed on a pulse amplitude modulation (PAM) chlorophyll fluorometer (Waltz GmbH) equipped with a WATER emitter-detector unit and analyzed using WinControl software (version 2.08, Waltz GmbH) according to Maxwell and Johnson (2000; and references therein). For daily analysis, 5–15 mL culture samples were dark adapted for 20 min at 20°C. Then the measuring light was turned on and the F_0 was recorded as the minimal fluorescence. During a saturating light flash, F_m° was recorded as the maximum fluorescence in the dark-adapted state. The maximum quantum yield of PSII ($F_v : F_m$) was calculated as $(F_m^\circ - F_0) : F_m^\circ$.

In addition to the daily analysis of $F_v : F_m$, NPQ was assessed in the exponential and stationary growth phase. Culture samples were dark adapted for 20 min, after which the $F_v : F_m$ was recorded as described above. Then, the actinic light of the WATER-PAM (blue light-emitting diode) was turned on and samples were exposed to high light (561 μmol photons m^{-2} s^{-1}) for 5 min. Directly after high-light exposure, the quantum yield of PSII (Φ_{PSII}) was determined by measuring F_t as the steady-state fluorescence prior to a saturating light flash and F'_m as the maximum fluorescence in the light. Φ_{PSII} was calculated as $(F'_m - F_t) : F'_m$. Then the measuring light was switched on and Φ_{PSII} was determined for every 5 min during a recovery period of 1 h. From the $F_v : F_m$ measurements at t = 0 and the Φ_{PSII} measurements at t = 5, total NPQ was calculated as $(F_m^\circ - F'_m) : F'_m$. Relaxation analysis was performed to estimate the contribution of slowly and rapidly relaxing NPQ. Relaxation of NPQ on a time scale of minutes is associated with photoprotective processes such as state transitions, relaxation of the xanthophyll pigment cycle, or other forms of thermal dissipation (Walters and Horton 1991; Demmig-Adams and Adams 1992; Maxwell and Johnson 2000). Processes that relax over a longer period of time (hours) are referred to as photoinhibition, i.e., damage to the reaction centers of PSII (Osmond 1994; Maxwell and Johnson 2000). To estimate photoprotection and photoinhibition, the recorded F'_m was corrected for baseline quenching by subtracting F_0 and was log transformed for further analysis. Transformed F'_m values of the final 40 min of the Φ_{PSII} recovery curve were extrapolated to calculate the value of F'_m that would have been attained if only slowly relaxing quenching was present in the light (F_m^r). Slowly relaxing non-photochemical quenching (NPQ_S) was then calculated as $(F_m^\circ - F_m^r) : F_m^r$ and fast-relaxing non-photochemical quenching (NPQ_F) as $(F_m^\circ : F'_m) - (F_m^\circ - F_m^r)$.

Elemental composition—For particulate organic carbon analysis, duplicate 20–35 mL culture samples were taken for each replicate culture and filtered onto 12 mm precombusted (4 h, 600°C) GF/F filters (Whatman), snap frozen in liquid nitrogen, and stored at −80°C until further analysis. For analysis, filters were acidified under HCl (37%) fumes for 4 h, dried overnight at 60°C, and wrapped in tin capsules (Elemental Microanalysis). Analysis was performed on a nitrogen and carbon analyzer type Flash EA™ 1112 (Interscience). Cellular C concentrations and C : Chl *a* were calculated using the cell density obtained by flow cytometry and the Chl *a* concentration obtained from the pigment analysis, respectively.

Pigment composition—Samples (25–55 mL) for pigment analysis were collected during the exponential and stationary growth phase for each replicate culture. Samples were filtered onto 25 mm GF/F filters (Whatman), snap frozen in liquid nitrogen, and stored at −80°C until further analysis. Pigments were quantified using high-performance liquid chromatography (HPLC) as described by Hooker et al. (2009). In short, filters were freeze-dried for 48 h and pigments were extracted in 3 mL 90% acetone (v : v, 48 h, 4°C). Detection of pigments was carried out using an HPLC (Waters 2695 separation module, 996 photodiode array detector) equipped with a Zorbax Eclipse extra dense bonding C_8 3.5 μm column (Agilent Technologies). Peaks were identified by retention time and diode array spectroscopy. Pigments were quantified using standards (DHI Lab products) of chlorophyll a_1, chlorophyll a_2, chlorophyll *b*, chlorophyll c_2, fucoxanthin, prasinoxanthin, diadinoxanthin (Dd), diatoxanthin (Dt), antheraxanthin (Ant), violaxanthin (Vio), and zeaxanthin (Zea). Hereafter, Chl *a* will refer to chlorophyll a_2 in *P. marinus* and to chlorophyll a_1 in *Ostreococcus* sp. and *T. oceanica*. The de-epoxidation state of the xanthophyll pigment cycle was calculated as (Ant + Zea) : (Vio + Ant + Zea) for *Ostreococcus* sp. and as Dt : (Dd + Dt) for *T. oceanica*.

Absorption spectra—Samples for phytoplankton pigment absorption spectra were taken during the exponential and stationary growth phase for each replicate culture. Pigment absorption spectra were determined on a Varian Cary 3E ultraviolet Vis spectrophotometer, equipped with an integrating sphere. Spectral values of the absorption coefficient were recorded every 1 nm between 300 and 800 nm. For analysis, 25–60 mL culture was filtered onto 25 mm GF/F filters (Whatman) and the transmission and reflection of the total particulate matter was determined according to Tassan and Ferrari (1995). The filter was then extracted in sodium hypochlorite (1% chlorine) to remove phytoplankton pigments and measured again to obtain the absorption of nonpigmented material (detritus). Phytoplankton absorption was calculated (β was set to 2) and normalized to Chl *a* concentrations to obtain the specific absorption coefficient by phytoplankton $a^*_{ph}(\lambda)$ (m^2 mg Chl

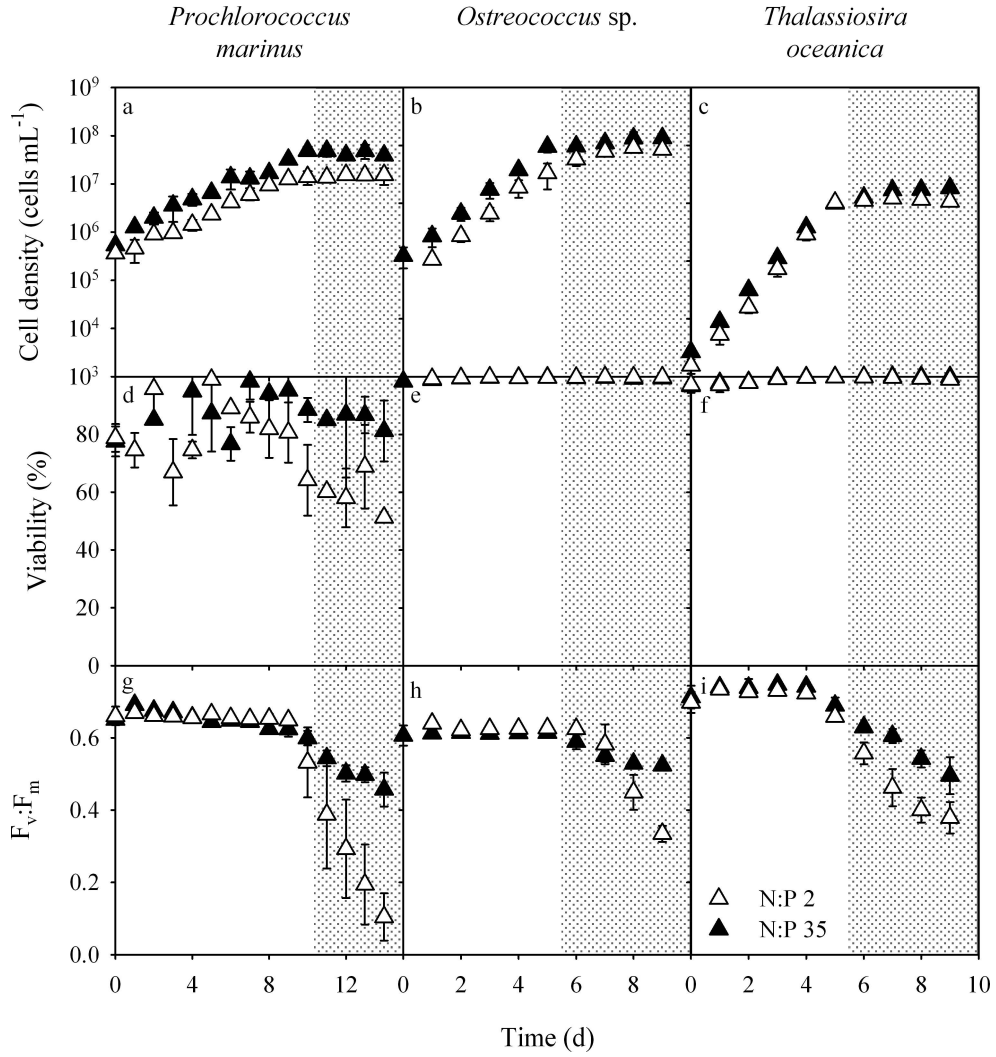

Fig. 2. Mean (± standard deviation, $n = 3$) (a–c) cell density, (d–f) viability, and (g–i) maximum quantum yield of photosystem II ($F_v : F_m$) for *Prochlorococcus marinus* ecotype MED4, *Ostreococcus* sp. clade B, and *Thalassiosira oceanica* grown at N : P 2 (white symbols) and N : P 35 (black symbols). Gray areas indicate the stationary growth phase in which cultures were either N (N : P 2) or P (N : P 35) starved.

a^{-1}). The spectrally weighted mean specific absorption coefficient $\bar{a}^*$ (m^2 mg Chl a^{-1}) was calculated by:

$$\bar{a}^* = \left(\frac{\sum_{700}^{400} a^*_{ph}(\lambda) E(\lambda)}{\sum_{700}^{400} E(\lambda)} \right) \quad (1)$$

with $E(\lambda)$ being the irradiance used in the incubator during the viability assay. The blue : red ratio was calculated by dividing the maximum $a^*_{ph}(\lambda)$ between 350–600 nm by the maximum $a^*_{ph}(\lambda)$ between 650–700 nm.

Statistical analysis—Differences between the two N : P ratios, the exponential (nutrient-replete) and stationary (nutrient-starved) growth phase, and the three phytoplankton species were statistically tested by analysis of variance using STATISTICA software (version 8.0 and 10.0, StatSoft). Before analysis, data were tested for normality and homogeneity of variances. Differences were considered significant when $p < 0.05$.

Results

Growth characteristics—Growth: The N : P ratio had no effect on the growth rates in *Prochlorococcus marinus* and *Ostreococcus* sp. (Fig. 2a,b). Growth rates were 0.41 ± 0.017 d^{-1} and 0.44 ± 0.011 d^{-1} in *P. marinus* and 0.94 ± 0.030 d^{-1} and 0.89 ± 0.088 d^{-1} in *Ostreococcus* sp. grown at N : P 2 and N : P 35, respectively. In *T. oceanica*, the growth rate was significantly higher at N : P 2 ($\mu = 1.40 \pm 0.084$ d^{-1}) compared with N : P 35 ($\mu = 1.26 \pm 0.06$ d^{-1}; $p < 0.014$; Fig. 2c). Overall, *T. oceanica* showed the highest growth rates, followed by *Ostreococcus* sp. and *P. marinus*,

respectively ($p < 0.001$). After exponential growth, *P. marinus* entered the stationary growth phase at t = 11 d, whereas *Ostreococcus* sp. and *T. oceanica* entered the stationary growth phase 4 d earlier, at t = 6 d (Fig. 2). All species, except for *P. marinus* at N : P 2, were able to maintain high cell densities for 28 d (separate cultures, data not shown). Regular nutrient analysis (data not shown) showed that the uptake of PO_4^{3-} halted with the onset of the stationary growth phase at N : P 2 (N starved) and PO_4^{3-} concentrations were typically depleted 1 d prior to the start of the stationary growth phase at N : P 35 (P starved). Nutrient-induced differences in cell size were not observed in *P. marinus* and *Ostreococcus* sp., but the cell size of *T. oceanica* increased during N starvation (4.7%) and decreased during P starvation (13%; $p < 0.005$; data not shown).

Viability at growth irradiance: In *P. marinus*, viability during the exponential and stationary growth phase ranged from 51% to 99% (Fig. 2d). Under nutrient-replete conditions, viability averaged at 81% ± 10.9% for N : P 2 and at 89% ± 7.8% for N : P 35 in the prokaryotic phytoplankton species. During N starvation, viability dropped significantly to 60% ± 7.2% in *P. marinus* ($p < 0.001$), whereas no differences in viability were observed between P-starved (85% ± 2.7%) and nutrient-replete conditions. Significant differences in viability were observed during nutrient-starved conditions, with lower viability at N : P 2 compared with N : P 35 ($p < 0.001$). In *Ostreococcus* sp. and *T. oceanica*, viability ranged from 96% to 100% (Fig. 2e,f). No significant differences between nutrient-replete and -starved conditions or between N : P ratios were observed for these eukaryotic phytoplankton species and viability was on average 99% ± 0.4% in *Ostreococcus* sp. and 99% ± 2.4% in *T. oceanica*. Overall, *Ostreococcus* sp. and *T. oceanica* showed significantly higher viability compared with *P. marinus* ($p < 0.05$).

Maximum quantum yield of PSII: The maximum quantum yield of PSII ($F_v : F_m$) was similar between the N : P ratios during exponential growth in all species, with the $F_v : F_m$ averaging at 0.656 ± 0.004 in *P. marinus*, 0.619 ± 0.011 in *Ostreococcus* sp., and 0.731 ± 0.009 in *T. oceanica* (Fig. 2g–i). At the onset of the stationary growth phase, $F_v : F_m$ decreased significantly during nutrient starvation ($p < 0.05$; Fig. 2g–i). The decrease in $F_v : F_m$ was significantly higher under N-starved conditions (N : P 2) compared with P-starved (N : P 35) conditions ($p < 0.05$; Fig. 2g–i). This was especially evident in *P. marinus*, in which the $F_v : F_m$ dropped by 84% at N : P 2 and by 24% at N : P 35. In the eukaryotic species, the $F_v : F_m$ dropped by 43–48% during N starvation compared with 15–33% during P starvation.

Responses to high-irradiance treatments—Viability during high-irradiance exposure: In response to high irradiance, viability decreased under all conditions in *P. marinus* (Fig. 3a–f). Viability loss in *P. marinus* was most evident within the first 30–60 min of high-irradiance exposure, with a significant decrease in viability between 18.6–66.7% ($p < 0.05$). After 60 min, further viability loss was limited under most conditions and at t = 240 min viability ranged from 28.9–61.9%. The response to high irradiance was uniform among the conditions and no significant effects N : P ratio or inhibitor treatment were found. Nutrient availability only played a role in the first 60 min of high-irradiance exposure at N : P 2, in which viability was significantly higher during N-starved conditions compared with replete conditions ($p < 0.05$).

Ostreococcus sp. showed higher viability during high-irradiance exposure compared with *P. marinus* and clear differences between the various nutrient conditions and inhibitor treatments were observed. In the control treatment (no inhibitor), viability did not significantly decrease during 4 h of high-irradiance exposure, except under nutrient-replete conditions at N : P 2 ($p < 0.01$; Fig. 3g,k). When the repair of damaged D1 proteins was blocked by the inhibitor Lincomycin, *Ostreococcus* sp. showed significantly higher viability loss compared with the control treatment ($p < 0.001$; Fig. 3h,l). In the Lincomycin treatment, viability decreased significantly after 60 min and 150 min of high-irradiance exposure at N : P 2 under nutrient-replete and N-starved conditions, respectively ($p < 0.04$). At N : P 35, viability decreased significantly after 120 min and 180 min of high-irradiance exposure under nutrient-replete and P-starved conditions, respectively ($p < 0.001$). *Ostreococcus* sp. showed lowest viability when PTOX-mediated alternative electron transport was blocked by the inhibitor Pgal. The viability of *Ostreococcus* sp. decreased significantly in the first 30 min of high-irradiance exposure during this treatment ($p < 0.05$; Fig. 3i,m). After 60 min of high-irradiance exposure, viability leveled off to around 38%, except under nutrient-replete conditions at N : P 35, at which viability decreased to 0% after 240 min of high-irradiance exposure. When the de-epoxidation of the xanthophyll pigment cycle was blocked by the inhibitor Dtt, viability loss during high-irradiance exposure was similar to the control treatment in *Ostreococcus* sp. (Fig. 3j,n). No effect of high-irradiance exposure was found in the Dtt treatment, except under nutrient-replete conditions at N : P 2, at which viability significantly decreased after 120 min of high-irradiance exposure ($p < 0.001$). When the different N : P ratios were compared in *Ostreococcus* sp., viability was significantly higher at N : P 2 in the Lincomycin and Pgal treatments, whereas viability was significantly higher at N : P 35 in the Control and Dtt treatments ($p < 0.05$ for nutrient-replete conditions). Overall, viability in *Ostreococcus* sp. was higher during nutrient-starved conditions compared with nutrient-replete conditions ($p < 0.05$).

T. oceanica showed significantly higher viability during high-irradiance exposure compared with *P. marinus* and *Ostreococcus* sp. (Fig. 3o–v). This was most evident in the control, Lincomycin, and Dtt treatments, where viability was not affected by high-irradiance exposure in *T. oceanica* (Fig. 3o,p,r–t,v). When PTOX-mediated alternative electron transport was blocked by the inhibitor Pgal, viability in *T. oceanica* decreased significantly upon high-irradiance exposure (Fig. 3q,u). At N : P 2, viability decreased after 120 min and 180 min of high-irradiance exposure under nutrient-replete and N-starved conditions, respectively ($p < 0.04$), whereas at N : P 35, viability decreased significantly

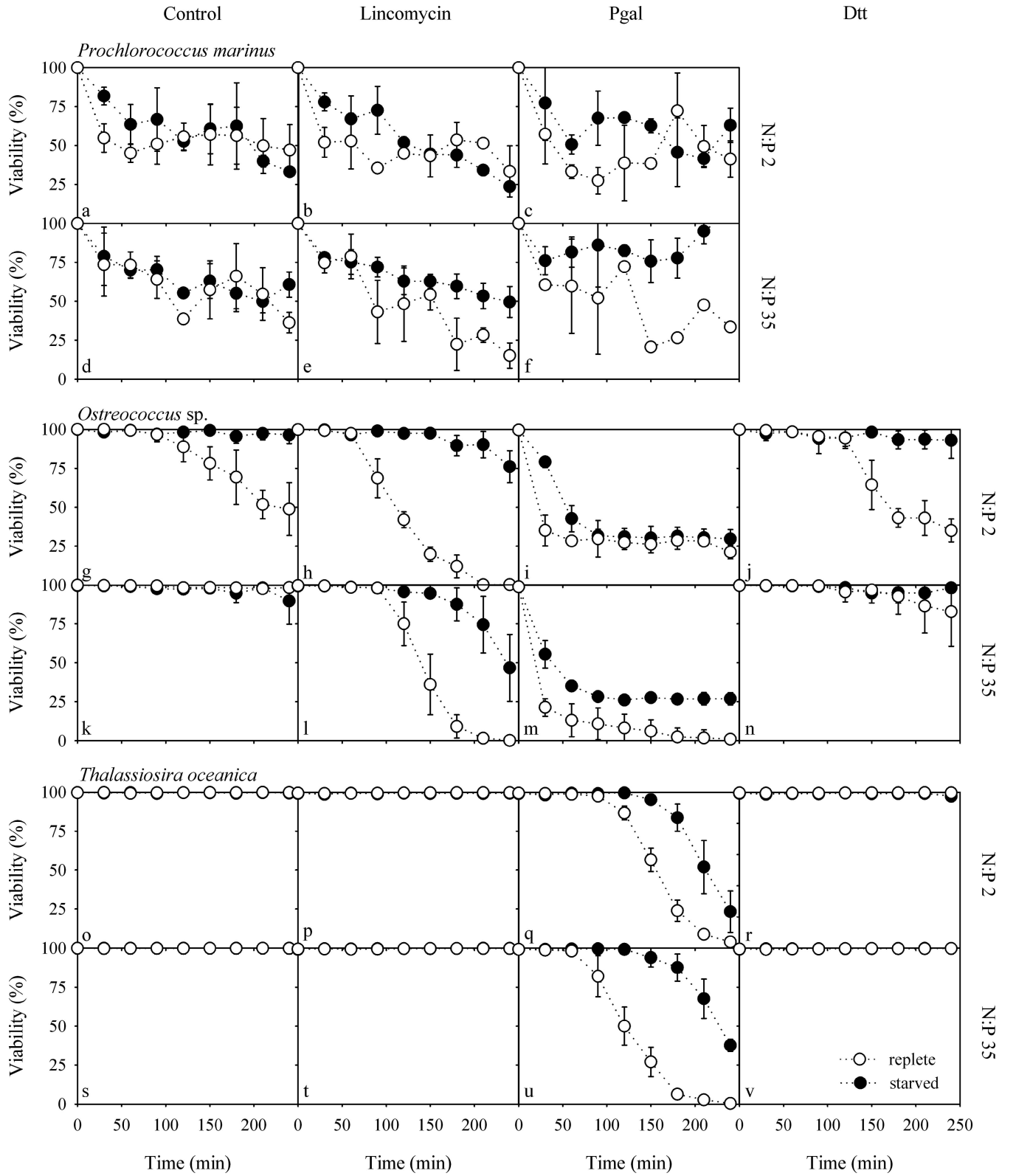

Fig. 3. Mean (± standard deviation, $n = 3$) viability (% of initial value) during high-irradiance exposure for (a–f) *P. marinus* ecotype MED4, (g–n) *Ostreococcus* sp. clade B, and (o–v) *T. oceanica* during nutrient-replete (white symbols) and -starved (black symbols) conditions. Inhibitor treatments (Control, Lincomycin, Pgal, and Dtt) and N : P ratios are presented in separate panels.

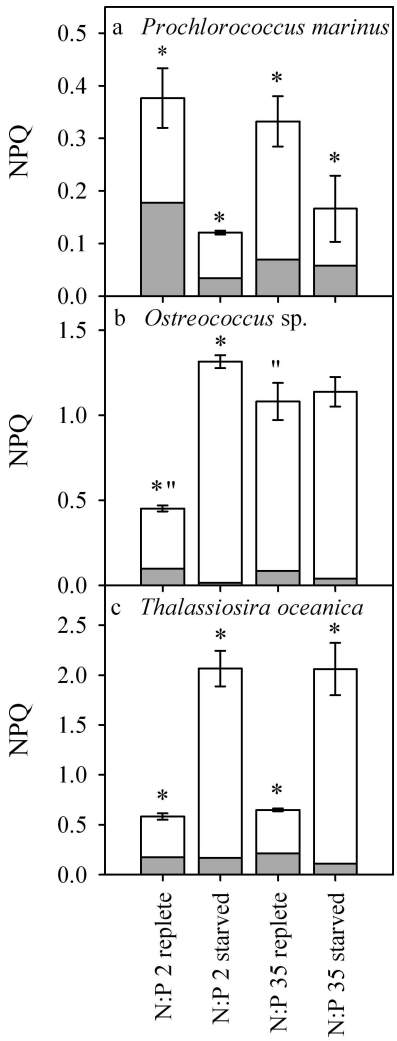

Fig. 4. Mean (± standard deviation, $n = 3$) non-photochemical quenching (NPQ) for (a) *P. marinus* ecotype MED4, (b) *Ostreococcus* sp. clade B, and (c) *T. oceanica* grown at N : P 2 and N : P 35 under nutrient-replete and -starved conditions. Slow- (gray) and fast- (white) relaxing NPQ are indicated separately. Significant differences ($p < 0.05$) between N : P ratios (") and nutrient-replete and -starved conditions (*) are indicated. Note that the scales of the y-axis are different between the panels.

after 90 min and 180 min of high-irradiance exposure under nutrient-replete and P-starved conditions, respectively ($p < 0.001$). Overall, viability in *T. oceanica* was higher during nutrient-starved conditions compared with nutrient-replete conditions ($p < 0.05$, Pgal treatment).

NPQ: NPQ decreased significantly during nutrient starvation in *P. marinus* ($p < 0.02$; Fig. 4a). This was related to a significant decrease in slow-relaxing NPQ ($p < 0.04$). No significant differences in NPQ were found between the N : P ratios in *P. marinus*.

In *Ostreococcus* sp., NPQ increased significantly during N starvation ($p < 0.001$), while no differences were observed in NPQ between nutrient-replete and P-starved conditions (Fig. 4b). The increase in NPQ during N starvation was accompanied by a significant decrease in slow-relaxing NPQ and a significant increase in fast-relaxing NPQ ($p < 0.01$). When the different N : P ratios were compared, *Ostreococcus* sp. showed significantly lower NPQ at N : P 2 compared with N : P 35 under nutrient-replete conditions ($p < 0.005$). During nutrient starvation, NPQ was similar between N : P 2 and N : P 35 in *Ostreococcus* sp.

In *T. oceanica*, NPQ increased significantly during both N and P starvation compared with nutrient-replete conditions ($p < 0.001$; Fig. 4c). This was related to a significant increase in fast-relaxing NPQ ($p < 0.001$). Differences in NPQ between the N : P ratios were not observed for *T. oceanica*. Overall, *T. oceanica* showed highest NPQ, followed by *Ostreococcus* sp. and *P. marinus*, respectively ($p < 0.001$), except in the exponential growth phase at N : P 35, at which *Ostreococcus* sp. showed significantly higher NPQ compared with *T. oceanica* ($p < 0.02$; Fig. 4).

(Photo)physiology during nutrient starvation—Elemental composition: The elemental composition was related to nutrient availability and N : P ratio in *P. marinus*, *Ostreococcus* sp., and *T. oceanica*. In *P. marinus*, the cellular C concentrations increased significantly during nutrient starvation ($p < 0.02$; Table 1). Related to the increase in cellular C, the C : Chl *a* ratio in *P. marinus* significantly increased during both N and P starvation ($p < 0.001$). When the different N : P ratios were compared, no differences in cellular C were observed in *P. marinus*, whereas the C : Chl *a* ratio was significantly lower at N : P 2 compared with N : P 35 ($p < 0.04$).

In *Ostreococcus* sp., cellular C concentrations were not affected by nutrient availability (Table 1). The C : Chl *a* ratio in *Ostreococcus* sp. was significantly higher at nutrient-replete compared with nutrient-starved conditions ($p < 0.001$), related to changes in cellular Chl *a* (Fig. 5). Comparison of the two N : P ratios showed that *Ostreococcus* sp. had higher cellular C concentrations at N : P 2 compared with N : P 35 ($p < 0.01$). The C : Chl *a* ratio was significantly higher at N : P 2 compared with N : P 35 during nutrient starvation ($p < 0.01$), whereas no difference in this ratio was observed in *Ostreococcus* sp. under nutrient-replete conditions.

In *T. oceanica*, cellular C concentrations increased significantly during N starvation ($p < 0.005$), whereas concentrations decreased during P starvation ($p < 0.04$; Table 1). Combined with the decrease in cellular Chl *a* in *T. oceanica* (Fig. 5), this resulted in a significant increase in the C : Chl *a* ratio during N starvation ($p < 0.001$), whereas this ratio was similar between nutrient-replete and P-starved conditions. When the N : P ratios were compared, *T. oceanica* showed lower cellular C concentrations at N : P 2 compared with N : P 35 during nutrient-replete growth ($p < 0.05$), whereas the opposite trend was observed during nutrient starvation ($p < 0.005$). The C : Chl *a* ratio was higher at N : P 2 compared with N : P 35 under nutrient-starved conditions ($p < 0.001$), but the C : Chl *a* ratio was similar during nutrient-replete growth in *T. oceanica*.

Pigment composition: Both light-harvesting and photoprotective pigmentation changed in response to nutrient starvation and N : P ratio. In the prokaryotic species *P.*

Table 1. Cellular composition. Mean (± standard deviation, $n = 3$) cellular carbon (C in pg cell^{-1}) and carbon to Chl *a* ratio (C : Chl *a* in w : w) for *Prochlorococcus marinus* ecotype MED4, *Ostreococcus* sp. clade B, and *Thalassiosira oceanica* grown at N : P 2 and N : P 35 under nutrient-replete and -starved conditions. Significant differences ($p < 0.05$) between N : P ratios (abc) and nutrient-replete and -starved conditions (*) are indicated.

	N : P 2		N : P 35	
	Replete	N starved	Replete	P starved
P. marinus				
C	0.21±0.017*	0.51±0.068*	0.18±0.082*	0.44±0.079*
C : Chl *a*	6.2±0.14a*	31.4±0.70b*	15.8±4.52a*	69.5±5.21b*
Ostreococcus sp.				
C	1.03±0.141c	0.95±0.043d	0.69±0.011c	0.67±0.006d
C : Chl *a*	36.4±1.25*	29.6±0.29e*	33.1±2.13*	23.9±1.13e*
T. oceanica				
C	14.0±2.03f*	20.0±1.07g*	17.7±1.35f*	13.8±0.90g*
C : Chl *a*	23.2±2.16*	84.3±13.83*h	25.9±5.55	22.2±3.13h

marinus, cellular chlorophyll *a* and *b* concentrations were similar between nutrient-replete and -starved conditions (Fig. 5a). Light-harvesting pigmentation was significantly different between the N : P ratios in *P. marinus*, with higher cellular chlorophyll *a* and *b* concentrations at N : P 2 compared with N : P 35 ($p < 0.05$; Fig. 5a). The photoprotective pigment zeaxanthin increased relative to Chl *a* by 7–8% during nutrient starvation ($p < 0.02$, not significant at N : P 35; Fig. 5b). The N : P ratio had no effect on the ratio of zeaxanthin to Chl *a* in *P. marinus*.

In the eukaryotic species *Ostreococcus* sp., cellular Chl *a* concentrations increased during nutrient starvation ($p < 0.05$, not significant for N : P 35; Fig. 5c). This trend was also observed for other light-harvesting pigments, such as chlorophyll *b* and prasinoxanthin (data not shown). The light-harvesting pigments were affected by N : P ratio, with higher cellular concentrations at N : P 2 compared with N : P 35 ($p < 0.05$, not significant for chlorophyll *a* and *b* during nutrient starvation). The total photoprotective pool of xanthophyll cycle pigments relative to Chl *a* increased significantly during nutrient starvation in *Ostreococcus* sp. ($p < 0.005$; Fig. 5d). During N starvation, this increase was related to a significant increase in antheraxanthin and zeaxanthin ($p < 0.001$), while during P starvation, the increase in the total xanthophyll cycle pigments pool was related to a significant increase in violaxanthin ($p < 0.004$; Fig. 5d). Consequently, the de-epoxidation state of the xanthophyll pigment cycle in *Ostreococcus* sp. was significantly higher under N-starved conditions (0.74 ± 0.056) compared with nutrient-replete conditions (0.14 ± 0.006) and no significant effect of P starvation was found on the de-epoxidation state (Fig. 5e). Differences in photoprotective pigmentation between the two N : P ratios were not observed under nutrient-replete conditions, whereas the photoprotective pigment pool and the de-epoxidation state were significantly higher at N : P 2 compared with N : P 35 during nutrient starvation ($p < 0.001$; Fig. 5e).

In *T. oceanica*, cellular Chl *a* concentrations decreased during N starvation ($p < 0.005$), while remaining similar to nutrient-replete conditions during P starvation (Fig. 5f). Other light-harvesting pigments, such as chlorophyll c_2 and fucoxanthin, showed a similar trend, but increased during nutrient starvation relative to Chl *a* ($p < 0.005$; data not shown). Differences in light-harvesting pigments between N : P ratios were not observed in *T. oceanica* under nutrient-replete conditions. During nutrient-starved conditions, cellular Chl *a*, chlorophyll c_2, and fucoxanthin concentrations were significantly lower at N : P 2 compared with N : P 35 ($p < 0.005$). Similar to *Ostreococcus* sp., the photoprotective pigment pool of *T. oceanica* increased significantly during nutrient starvation ($p < 0.05$; Fig. 5g). Both the cellular concentrations and the relative concentration to Chl *a* of diadinoxanthin and diatoxanthin increased significantly during N and P starvation ($p < 0.05$). This related to a significant increase in the de-epoxidation state of the xanthophyll pigment cycle ($p < 0.02$; Fig. 5h). In *T. oceanica*, the xanthophyll cycle pigments per Chl *a* ratio was similar between the N : P ratios under nutrient-replete conditions. During nutrient starvation, the photoprotective pigment pool per Chl *a* was significantly higher at N : P 2 compared with N : P 35 ($p < 0.03$), which related to the differences observed in cellular Chl *a* (Fig. 5f,g). No significant differences in de-epoxidation state of the xanthophyll pigment cycle between the N : P ratios were observed (Fig. 5h).

Absorption spectra: Absorption properties of the different phytoplankton species were influenced by both nutrient availability and N : P ratios (Table 2). In *P. marinus*, the spectrally weighted mean absorption coefficient ($\bar{a}^*$) increased significantly during nutrient starvation compared with nutrient-replete conditions ($p < 0.001$). In contrast, $\bar{a}^*$ decreased during nutrient starvation in *Ostreococcus* sp. ($p < 0.01$, not significant at N : P 2). Similar to *P. marinus*, $\bar{a}^*$ increased significantly during N starvation in *T. oceanica* ($p < 0.05$), but no significant differences in $\bar{a}^*$ were observed between nutrient-replete and P-starved conditions. When the different N : P ratios were compared, $\bar{a}^*$ was significant lower at N : P 2 compared with N : P 35 in *P. marinus* and *T. oceanica* ($p < 0.01$, except for *T. oceanica* under nutrient-replete conditions). In contrast, no significant effect of N : P ratio on $\bar{a}^*$ was observed in *Ostreococcus* sp. Overall, *Ostreococcus* sp. showed the highest $\bar{a}^*$

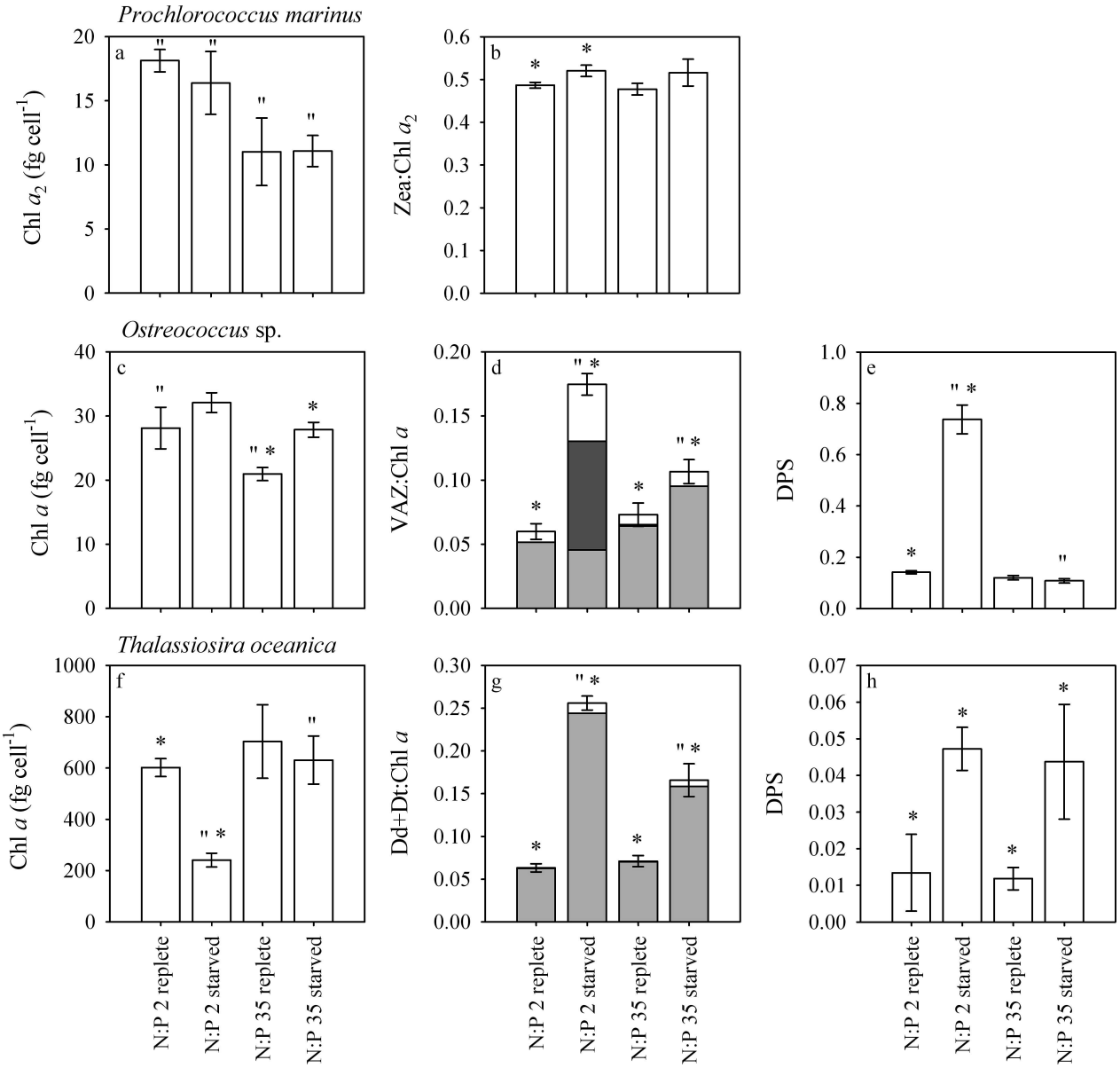

Fig. 5. Mean (± standard deviation, $n = 3$) cellular Chl *a* concentrations and the photoprotective pigments per Chl *a* ratio for *P. marinus* ecotype MED4, *Ostreococcus* sp. clade B, and *T. oceanica* grown at N : P 2 and N : P 35 under nutrient-replete and -starved conditions. For *Ostreococcus* sp. and *T. oceanica*, the de-epoxidation state (DPS) of the xanthophyll pigment cycle is also given. The xanthophyll cycle pigments violaxanthin (light gray), antheraxanthin (dark gray), and zeaxanthin (white) in (d) *Ostreococcus* sp. and diadinoxanthin (light gray) and diatoxanthin (white) in (g) *T. oceanica* are separately indicated. Significant differences ($p < 0.05$) between N : P ratios (") and nutrient-replete and -starved conditions (*) are indicated. Abbreviations: Chl *a*, chlorophyll *a*; Zea, zeaxanthin; VAZ, violaxanthin + antheraxanthin + zeaxanthin; Dd, diadinoxanthin; and Dt, diatoxanthin.

compared with the other species, except under P starvation, at which *P. marinus* showed the highest $\bar{a}^*$ ($p < 0.001$).

The blue : red ratio was not significantly affected by nutrient availability and N : P ratio in *P. marinus* and *Ostreococcus* sp. (Table 2). In *T. oceanica*, the blue : red ratio increased under nutrient-starved conditions ($p < 0.005$, not significant at N : P 35). In addition, the blue : red ratio was significantly higher at N : P 2 compared with N : P 35 in *T. oceanica* ($p < 0.001$). Overall, *P. marinus* and *Ostreococcus* sp. showed the highest blue : red ratios, followed by *T. oceanica* ($p < 0.01$).

Discussion

In the present study, the viability of different oceanic phytoplankton species was investigated to determine the relative importance of irradiance and nutrient conditions in phytoplankton viability loss. It was previously suggested that both the depth and geographic distribution of viable *Prochlorococcus*, *Synechococcus*, and eukaryotic phytoplankton cells in open oceans is related to irradiance and nutrient availability (Agustí 2004; Alonso-Laita and Agustí 2006; Llabrés and Agustí 2006). This study showed that

Table 2. Absorption spectra. Mean (± standard deviation, $n = 3$) spectrally weighted mean specific absorption coefficient $\bar{a}^*$ (m^2 mg Chl a^{-1}) and blue : red ratio for *P. marinus* ecotype MED4, *Ostreococcus* sp. clade B, and *T. oceanica* grown at N : P 2 and N : P 35 under nutrient-replete and -starved conditions. Significant differences ($p < 0.05$) between N : P ratios (abc) and nutrient-replete and -starved conditions (*) are indicated.

	N : P 2		N : P 35	
	Replete	N starved	Replete	P starved
P. marinus				
$\bar{a}^*$	$0.011 \pm 1.09 \times 10^{-3}$a*	$0.020 \pm 2.28 \times 10^{-4}$b*	$0.019 \pm 2.71 \times 10^{-3}$a*	$0.030 \pm 2.23 \times 10^{-3}$b*
Blue : red	2.00±0.110c	1.92±0.056d	1.86±0.077c	1.76±0.109d
Ostreococcus sp.				
$\bar{a}^*$	$0.031 \pm 2.99 \times 10^{-3}$	$0.026 \pm 5.74 \times 10^{-4}$	$0.038 \pm 6.04 \times 10^{-3}$*	$0.025 \pm 9.11 \times 10^{-4}$*
Blue : red	1.90±0.042	1.91±0.080	1.90±0.113	1.77±0.096
T. oceanica				
$\bar{a}^*$	$0.016 \pm 1.13 \times 10^{-3}$*	$0.020 \pm 1.88 \times 10^{-3}$e*	$0.014 \pm 2.69 \times 10^{-3}$	$0.012 \pm 1.55 \times 10^{-3}$e
Blue : red	1.23±0.021f*	1.46±0.069g*	1.17±0.025f	1.41±0.173g

high-irradiance exposure can indeed lead to viability loss in oceanic phytoplankton. Similar to species-specific differences observed in the North Atlantic Ocean and other oligotrophic regions (Sommaruga et al. 2005; Llabrés and Agustí 2006; Agustí and Llabrés 2007), viability loss during high-irradiance exposure was higher in *Prochlorococcus marinus* compared with the eukaryotic species. Additional exposure to UVR may enhance photoinhibition and viability loss in specific phytoplankton species. For example, *Prochlorococcus* spp. shows a high sensitivity to UVR (Kulk et al. 2013), which could explain the low viability observed in this species near the surface of open oligotrophic oceans (Alonso-Laita and Agustí 2006; Agustí and Llabrés 2007). However, the present study showed that nutrient availability alone would not account for significant viability loss in oceanic phytoplankton species, except in *P. marinus* at low NH_4^+ availability. In the upper mixed layer of open oligotrophic oceans, phytoplankton can experience high (dynamic) irradiance conditions in combination with low nutrient availability. It has been suggested that these co-occurring conditions increase photoinhibition and viability loss in natural communities (Lesser et al. 1994; Llabrés and Agustí 2006; Franklin et al. 2009). However, the present study showed that *P. marinus*, *Ostreococcus* sp., and *T. oceanica* are actually less susceptible to both photoinhibition and viability loss during high-irradiance exposure when nutrient availability is low. Similar responses were observed for the Antarctic diatom *Chaetoceros brevis* during N, P, and iron (Fe) starvation (Van de Poll et al. 2005) and *Emiliania huxleyi* during N starvation (Loebl et al. 2010). The lower photoinhibition and viability loss during high-irradiance exposure at low-nutrient availability was related to a reduced light-harvesting capacity and/or enhanced photoprotection, although different photoregulating mechanisms were involved in *P. marinus*, *Ostreococcus* sp., and *T. oceanica*.

The response of *P. marinus* to both nutrient starvation and high-irradiance exposure was clearly different from the other two species. In all treatments, viability loss of *P. marinus* was highest in the first 30–60 min of high-irradiance exposure. Photoinhibition and viability loss during high-irradiance exposure decreased during nutrient starvation in *P. marinus*, although the differences in viability loss were less evident during P starvation. In *P. marinus*, the lower sensitivity to high-irradiance intensities during nutrient starvation was not associated with changes in pigmentation. Moreover, the absorption per Chl *a* increased considerably during nutrient starvation. A similar increase in absorption was observed during high-light acclimation in high-light-adapted ecotypes of *Prochlorococcus* (Partensky et al. 1993; Moore and Chisholm 1999; Kulk et al. 2011). The unchanged levels of Chl *a* and the increase in absorption per Chl *a* therefore suggest that light-harvesting capacity increased during nutrient starvation in *P. marinus*. However, photoinhibition and viability loss during high-irradiance exposure did not increase after nutrient starvation in *P. marinus*, suggesting that additional photophysiological changes must have occurred during nutrient starvation. Because viability loss during high-irradiance exposure was not increased when PTOX-mediated alternative electron transport downstream of PSII was inhibited, the changes in photophysiology during nutrient starvation were most likely related to PSII functioning. The maximum quantum yield of PSII ($F_v : F_m$) decreased considerably during nutrient starvation in *P. marinus*. In several ecotypes of *Prochlorococcus*, a similar decrease in $F_v : F_m$ during N starvation was observed (Steglich et al. 2001; Lindell et al. 2002) and paralleled a decrease in functional PSII reaction centers in a low-light–adapted ecotype of *Prochlorococcus* (Steglich et al. 2001). It is likely that a similar decline in functional PSII reaction centers occurred during nutrient starvation in *P. marinus*, although differences among *Prochlorococcus* ecotypes cannot be excluded. This potential loss of functional PSII reaction centers is not associated with photoinhibition at growth irradiance, because photoinhibition during high-irradiance exposure decreased when nutrient availability was low and the inhibition of D1 repair had no effect on photoinhibition (data not shown) and viability loss during high-irradiance exposure. Possibly, the loss of functional PSII reaction centers is caused by the disconnection of light-harvesting complexes (Riethman and Sherman 1988; Steglich et al. 2001; Behrenfeld and Milligan 2013). This has been observed for

several phytoplankton species during Fe starvation (Greene et al. 1991; for a review *see* Behrenfeld and Milligan 2013) and would explain why levels of cellular Chl *a* remained unchanged during nutrient starvation in *P. marinus*.

The lower sensitivity to high-irradiance exposure in *Ostreococcus* sp. was observed under both N and P starvation. The increase in cellular Chl *a* coincided with a decrease in chlorophyll absorption, suggesting that the light-harvesting capacity was little affected by nutrient starvation in *Ostreococcus* sp. Generally the Chl *a* concentration decreases, while chlorophyll specific absorption increases during nutrient starvation in eukaryotic phytoplankton species (Geider et al. 1993; Berges and Falkowski 1998; Loebl et al. 2010), but a similar response to *Ostreococcus* sp. was found in *Dunalliela tertiolecta* during P starvation (La Roche et al. 1993). When photoprotection is considered in *Ostreococcus* sp., clear differences between N and P starvation were observed. During N starvation, the concentration as well as the de-epoxidation state of the xanthophyll pigment cycle increased, similar to other phytoplankton species (Geider et al. 1993; Berges and Falkowski 1998; Franklin et al. 2012). The increased de-epoxidation state of the xanthophyll pigment cycle coincided with an increase in the dissipation of excess energy during high-irradiance exposure (fast-relaxing NPQ) and might explain why the $F_v : F_m$ decreased in *Ostreococcus* sp. In contrast to N starvation, the de-epoxidation state of the xanthophyll pigment cycle did not increase during P starvation. However, fast-relaxing NPQ was at similar levels during N and P starvation. Therefore, another photoregulating mechanism contributing to fast-relaxing NPQ may have played an important role during P starvation in *Ostreococcus* sp. It was earlier suggested that PTOX-mediated electron transport regulates light-harvesting energy in oceanic ecotypes of *Ostreococcus* spp. (Cardol et al. 2008), which is also evident in the present study from the significant decrease in viability during high-irradiance exposure when this process was inhibited by Pgal. Since viability loss was higher when *Ostreococcus* sp. was grown at N : P 35 compared with N : P 2, it seems that PTOX-mediated electron transport instead of the xanthophyll pigment cycle played a more important role in photoregulation during low P availability.

T. oceanica showed lowest viability loss during high-irradiance exposure. In this species, the lower sensitivity to high irradiance during nutrient starvation was evident from reduced photoinhibition (P starvation) and reduced viability loss when PTOX-mediated alternative electron transport was inhibited (both N and P starvation). This lower photoinhibition and viability loss was associated with an increase in photoprotection by the xanthophyll pigment cycle during nutrient starvation. The xanthophyll cycle pigments increased relative to Chl *a* and per cell during nutrient starvation in *T. oceanica*. Moreover, the de-epoxidation state of the xanthophyll pigment cycle increased during nutrient starvation. These changes in photoprotective pigmentation were earlier observed in other diatom species, such as *Phaedactylum tricornutum* (Geider et al. 1993) and *C. brevis* (Van de Poll et al. 2005), during both N and P starvation. The increased de-epoxidation state of the xanthophyll pigment cycle during nutrient starvation in *T. oceanica* coincided with a strongly enhanced dissipation of excess energy by NPQ. Enhanced fast-relaxing NPQ could explain the decrease in $F_v : F_m$ observed during nutrient starvation in *T. oceanica* and other diatom species (Geider et al. 1993; Van de Poll et al. 2005). Although PTOX-mediated alternative electron transport was present in *T. oceanica* and it clearly supported survival during high-irradiance exposure, it is unclear whether this mechanism functions in a similar fashion as compared to *Ostreococcus* sp. (this study; Cardol et al. 2008). In *Thalassiosira pseudonana*, alternative electron transport routes do seem to play an important role in addition to NPQ processes in the prevention of photoinhibition (Waring et al. 2010). In addition to enhanced photoprotection, *T. oceanica* reduced light-harvesting capacity during N starvation by a decrease in cellular Chl *a* concentrations. This is a common response to nutrient starvation in eukaryotic phytoplankton (Geider et al. 1993; Berges and Falkowski 1998; Loebl et al. 2010), but was not observed during P starvation in *T. oceanica*. It is possible that during P starvation, selective degradation of membrane proteins occurred, rather than proteins associated with light-harvesting complex and the Calvin cycle as observed during N starvation (Plumley and Schmidt 1989; Geider et al. 1993; Berges and Falkowski 1998). This is partly confirmed by the lower decrease in cellular N during P starvation compared with N starvation in *T. oceanica* (data not shown). Changes in chlorophyll absorption were not observed in *T. oceanica*, suggesting that the alterations in pigmentation were the main factor influencing light-harvesting capacity during nutrient starvation.

The present study showed that high-irradiance exposure can cause considerable viability loss in phytoplankton in the upper mixed layer of open oligotrophic oceans. However, low-nutrient availability does not necessarily decrease viability in oceanic phytoplankton. Instead, it may have a positive feedback on the high-irradiance response of oceanic phytoplankton. *P. marinus*, *Ostreococcus* sp., and *T. oceanica* showed reduced sensitivity to high-irradiance exposure when nutrient availability was low, although species-specific differences were observed. In *P. marinus*, the lower sensitivity to high-irradiance intensities at low-nutrient availability was related to changes in a photoregulating process prior to electron transport that did not involve changes in pigmentation, possibly the decoupling of antenna complexes from PSII. In *Ostreococcus* sp., the reduced high-irradiance sensitivity was related to enhanced photoprotection by the xanthophyll pigment cycle or alternative electron transport, depending on the limiting nutrient. In *T. oceanica*, enhanced photoprotection by the xanthophyll pigment cycle ensured lower sensitivity to high-irradiance exposure when nutrient availability was low. Ultimately, low-nutrient availability may determine the distribution and primary production of oceanic phytoplankton, but high PAR and UVR exposure, grazing pressure, or viral infection rather than nutrient availability governs viability loss of phytoplankton in open oligotrophic oceans. Climate change may increase the average irradiance intensity oceanic phytoplankton experience and may simultaneously decrease nutrient availability due to enhanced thermal

stratification. This will influence phytoplankton viability loss, as demonstrated by the present study. However, the interplay between these changing conditions needs to be addressed in more detail to understand and predict the consequences of climate change for phytoplankton productivity and community composition in open oceans.

Acknowledgments

We thank S. Ossebaar for analysis of particulate organic carbon. We would also like to thank two anonymous reviewers for their helpful comments. This work was supported by the Netherlands Organization for Scientific Research (N.W.O.), grant numbers 817.01.009 (G.K.) and 839.08.422 (W.H.P.).

References

Agustí, S. 2004. Viability and niche segregation of *Prochlorococcus* and *Synechococcus* cells across the Central Atlantic Ocean. Aquat. Microb. Ecol. **36:** 53–59.

———, and M. Llabrés. 2007. Solar radiation-induced mortality of marine pico-phytoplankton in the oligotrophic ocean. Photochem. Photobiol. **83:** 793–801.

———, and M. C. Sánchez. 2002. Cell viability in natural phytoplankton communities quantified by a membrane permeability probe. Limnol. Oceanogr. **47:** 818–828.

Alonso-Laita, P., and S. Agustí. 2006. Contrasting patterns of phytoplankton viability in the subtropical NE Atlantic Ocean. Aquat. Microb. Ecol. **43:** 67–78.

Aro, E. M., I. Virgin, and B. Andersson. 1993. Photoinhibition of photosystem II. Inactivation, protein damage and turnover. Biochem. Biophys. Acta **1143:** 113–134.

Bailey, S., and others. 2008. Alternative photosynthetic electron flow to oxygen in marine *Syenchococcus*. Biochem. Biophys. Acta **1777:** 269–276.

Behrenfeld, M. J., and A. J. Milligan. 2013. Photophysiological expression of iron stress in phytoplankton. Annu. Rev. Mar. Sci. **5:** 217–246.

———, and others. 2006. Climate-driven trends in contemporary ocean productivity. Nature **444:** 753–755.

Berges, J. A., D. O. Charlebois, D. C. Mauzerall, and P. G. Falkowski. 1996. Differential effects of nitrogen limitation on photosynthetic efficiency of photosystem I and II in microalgae. Plant Physiol. **110:** 689–696.

———, and P. G. Falkowski. 1998. Physiological stress and cell death in marine phytoplankton: Induction of proteases in response to nitrogen or light limitation. Limnol. Oceanogr. **43:** 129–135.

Boyd, P. W., and S. C. Doney. 2002. Modelling regional responses by marine pelagic ecosystems to global climate change. Geophys. Res. Lett. **29:** 10.1029, doi:10.1029/2001GL014130

Brussaard, C. P. D., A. A. M. Noordeloos, and R. Riegman. 1997. Autolysis kinetics of the marine diatom *Ditylum brightwellii* (Bacillariophyceae) under nitrogen and phosphorus limitation and starvation. J. Phycol. **33:** 980–987.

———, and R. Riegman. 1998. Influence of bacteria on phytoplankton cell mortality with phosphorus or nitrogen as the alga-growth-limiting nutrient. Aquat. Microb. Ecol. **14:** 271–280.

Cardol, P., and others. 2008. An original adaptation of photosynthesis in the marine green alga *Ostreococcus*. Proc. Natl. Acad. Sci. USA **105:** 7881–7886.

Cavender-Bares, K. K., D. M. Karl, and S. W. Chisholm. 2001. Nutrient gradients in the western North Atlantic Ocean: Relationship to microbial community structure and comparison to patterns in the Pacific Ocean. Deep-Sea Res. I **48:** 2373–2395.

Chisholm, S. W. 1992. Phytoplankton size, p. 213–237. *In* P. G. Falkowski and A. D. Woodhead [eds.], Primary productivity and biogeochemical cycles in the sea. Plenum.

Davey, M., G. A. Tarran, M. M. Mills, C. Ridame, R. J. Geider, and J. La Roche. 2008. Nutrient limitation of picophytoplankton photosynthesis and growth in the tropical North Atlantic. Limnol. Oceanogr. **53:** 1722–1733, doi:10.4319/lo.2008.53.5.1722

Demir-Hilton, E., S. Sudek, M. L. Cuvelier, C. L. Gentemann, J. P. Zehr, and A. Z. Worden. 2011. Global distribution patterns of distinct clades of the photosynthetic picoeukaryote *Ostreococcus*. ISME J. **5:** 1095–1107.

Demmig-Adams, B., and W. W. Adams. 1992. Photoprotection and other responses of plants to high light stress. Annu. Rev. Plant Phys. **43:** 599–626.

Dimier, C., S. Giovanni, T. Ferdinando, and C. Brunet. 2009. Comparative ecophysiology of the xanthophyll cycle in six marine phytoplanktonic species. Protist **160:** 397–411.

DuRand, M. D., R. J. Olson, and S. W. Chisholm. 2001. Phytoplankton population dynamics at the Bermuda Atlantic Time-series station in the Sargasso Sea. Deep-Sea Res. II **48:** 1983–2003.

Franklin, D. J., R. L. Airs, M. Fernandes, T. G. Bell, R. J. Bongaerts, J. A. Berges, and G. Malin. 2012. Identification of senescence and death in *Emiliania huxleyi* and *Thalassiosira pseudonana*: Cell staining, chlorophyll alterations, and dimethylsulfoniopropionate (DMSP) metabolism. Limnol. Oceanogr. **57:** 305–317.

———, C. J. Choi, C. Hughes, G. Malin, and J. A. Berges. 2009. Effect of dead phytoplankton cells on the apparent efficiency of photosystem II. Mar. Ecol. Prog. Ser. **382:** 35–40.

Gechev, T. S., F. Van Breusegem, J. M. Stone, I. Denev, and C. Laloit. 2006. Reactive oxygen species as signals that modulate plant stress responses and programmed cell death. BioEssays **28:** 1091–1101.

Geider, R. J., J. La Roche, R. M. Greene, and M. Oloizola. 1993. Response of the photosynthetic apparatus of *Phaeodactylum tricornutum* (Bacillariophyceae) to nitrate, phosphate, or iron starvation. J. Phycol. **29:** 755–766.

Graziano, L. M., R. J. Geider, W. K. W. Li, and M. Olaizola. 1996. Nitrogen limitation of North Atlantic phytoplankton: Analysis of physiological condition in nutrient enrichment experiments. Aquat. Microb. Ecol. **11:** 53–64.

Greene, R. M., R. J. Geider, and P. G. Falkowski. 1991. Effects of iron limitation on photosynthesis in a marine diatom. Limnol. Oceanogr. **36:** 1772–1782.

Herzig, R., and P. G. Falkowski. 1989. Nitrogen limitation in *Isochrysis galbana* (Haptophyceae). I. Photosynthetic energy conversion and growth efficiencies. J. Phycol. **25:** 462–471.

Hooker, S. B., and others. 2009. The third SeaWiFS HPLC Analysis Round-Robin Experiment (SeaHARRE-3). NASA Technical Memo 2009-215849. NASA Goddard Space Flight Center.

Johnson, Z. I., E. R. Zinser, A. Coe, N. P. McNulty, E. M. S. Woodward, and S. W. Chisholm. 2006. Niche partitioning among *Prochlorococcus* ecotypes along ocean-scale environmental gradients. Nature **311:** 1737–1740.

Karl, D., R. Letelier, L. Tupas, J. Dore, J. Cristian, and D. Hebel. 1997. The role of nitrogen fixation in biogeochemical cycling in the subtropical North Pacific Ocean. Nature **388:** 533–538.

Keller, M. D., R. C. Selvin, W. Claus, and R. R. L. Guillard. 1987. Media for the culture of oceanic ultraphytoplankton. J. Phycol. **23:** 633–638.

Kirk, T. O. 2010. Light and photosynthesis in aquatic ecosystems, 3rd ed. Cambridge Univ. Press.

Kulk, G., P. De Vries, W. H. Van de Poll, R. J. W. Visser, and A. G. J. Buma. 2013. Temperature-dependent photoregulation in oceanic phytoplankton during excessive irradiance exposure, p. 209–228. *In* Z. Dubinsky [ed.], Photosynthesis. InTech.

———, W. H. Van de Poll, R. J. W. Visser, and A. G. J. Buma. 2011. Distinct differences in photoacclimation potential between prokaryotic and eukaryotic oceanic phytoplankton. J. Exp. Mar. Biol. Ecol. **398:** 63–72.

La Roche, J., R. J. Geider, L. M. Graziano, H. Murray, and K. Lewis. 1993. Induction of specific proteins in eukaryotic algae grown under iron-, phosphorus-, or nitrogen-deficient conditions. J. Phycol. **29:** 767–777.

Lesser, M. P., J. J. Cullen, and P. J. Neale. 1994. Carbon uptake in a marine diatom during acute exposure to ultraviolet B radiation: Relative importance of damage and repair. J. Phycol. **30:** 183–192.

Li, W. K. W. 1994. Primary production of prochlorophytes, cyanobacteria, and eukaryotic ultraphytoplankton—measurements from flow cytometric sorting. Limnol. Oceanogr. **39:** 169–175.

Lindell, D., and others. 2002. Nitrogen stress response of *Prochlorococcus* strain PCC 9511 (oxyphotobacteria) involves constrating regulation of *ntcA* and *amt1*. J. Phycol. **38:** 1113–1124.

Llabrés, M., and S. Agustí. 2006. Picophytoplankton cell death induced by UV radiation: Evidence of oceanic Atlantic communities. Limnol. Oceanogr. **51:** 21–29.

Loebl, M., A. M. Cockshutt, D. A. Campbell, and Z. V. Finkel. 2010. Physiological basis of high resistance to photoinhibition under nitrogen depletion in *Emiliania huxleyi*. Limnol. Oceanogr. **55:** 2150–2160.

Maxwell, K., and G. N. Johnson. 2000. Chlorophyll fluorescence—a practical guide. J. Exp. Bot. **51:** 659–668.

Moore, L. R., and S. W. Chisholm. 1999. Photophysiology of the marine cyanobacterium *Prochlorococcus*: Ecotypic differences among cultures isolates. Limnol. Oceanogr. **44:** 628–638.

———, G. Rocap, and S. W. Chisholm. 1998. Physiology and molecular phylogeny of coexisting *Prochlorococcus* ecotypes. Nature **393:** 464–467.

Murphy, J., and J. P. Riley. 1962. A modified single solution method for determination of phosphate in natural waters. Anal. Chim. Acta **26:** 31–36.

Olaizola, M., J. La Roche, Z. Kolber, and P. G. Falkowski. 1994. Non-photochemical fluorescence quenching and the diadinoxanthin cycle in a marine diatom. Photosynth. Res. **41:** 357–370.

Osmond, C. B. 1994. What is photoinhibition? Some insights from comparisons of sun and shade plants, p. 1–24. *In* N. R. Baker and J. R. Bowyer [eds.], Photoinhibition of photosynthesis: From molecular mechanisms to the field. Bios Scientific Publishers.

Partensky, F., N. Hoepffner, W. K. W. Li, O. Ulloa, and D. Vaulot. 1993. Photoacclimation of *Prochlorococcus* sp. (prochlorophyta) strains isolated from the North Atlantic and the Mediterranean Sea. Plant Physiol. **101:** 285–296.

Peperzak, L., and C. P. D. Brussaard. 2011. Flow cytometric applicability of fluorescent vitality probes on phytoplankton. J. Phycol. **47:** 692–702.

Plumley, F. G., and G. W. Schmidt. 1989. Nitrogen-dependent regulation of the photosynthetic gene expression. Proc. Natl. Acad. Sci. USA **86:** 2678–2682.

Raven, J. A. 2011. The cost of photoinhibition. Physiol. Plant. **142:** 87–104.

Riethman, H. C., and L. A. Sherman. 1988. Purification and characterization of an iron stress-induced chlorophyll-protein from the cyanobacterium *Anacystis nidulans* R2. Biochim. Biophys. Acta **935:** 141–151.

Six, C., C. Finkel, A. J. Irwin, and D. A. Campbell. 2007. Light variability illuminates niche-partitioning among marine picocyanobacteria. PLoS One **12:** e1341, doi:10.1371/journal.pone.0001341

Sommaruga, R., J. S. Hofer, L. Alonso-Sáez, and J. M. Gasol. 2005. Differential sunlight sensitivity of picophytoplankton from surface Mediterranean coastal waters. Appl. Environ. Microb. **71:** 2154–2157.

Steglich, C., and others. 2001. Nitrogen deprivation strongly affects photosystem II but not phycoerythrin level in the divinyl-chlorophyll *b*-containing cyanobacterium *Prochlorococcus marinus*. Biochim. Biophys. Acta **1503:** 341–349.

Tassan, S., and G. M. Ferrari. 1995. Proposal for the measurement of backward and total scattering by mineral particles suspended in water. Appl. Opt. **34:** 8345–8353.

Van de Poll, W.H.A.C. Alderkamp, P. J. Janknegt, J. Roggeveld, and A. G. J. Buma. 2006. Photoacclimation modulates excessive photosynthetically active and ultraviolet radiation effects in a temperate and an Antarctic marine diatom. Limnol. Oceanogr. **51:** 1239–1248, doi:10.4319/lo.2006.51.3.1239

———, M. A. Van Leeuwe, J. Roggeveld, and A. G. J. Buma. 2005. Nutrient limitation and high irradiance acclimation reduce Par and UV-induced viability loss in the Antarctic diatom *Chaetoceros brevis* (Bacillariophyceae). J. Phycol. **41:** 840–850.

———, G. Kulk, K. R. Timmermans, C. P. D. Brussaard, H. J. Van de Woerd, M. J. Kehoe, K. D. A. Majoica, R. J. W. Visser, P. D. Rozema, and A. G. J. Buma. 2013. Phytoplankton chlorophyll *a* biomass, composition, and productivity along a temperature and stratification gradient in the northeast Atlantic Ocean. Biogeosciences **10:** 4227–4240, doi:10.5194/bg-10-4227-2013

———, R. J. W. Visser, and A. G. J. Buma. 2007. Acclimation to a dynamic irradiance regime changes excessive irradiance sensitivity of *Emiliania huxleyi* and *Thalassiosira weissflogii*. Limnol. Oceanogr. **52:** 1430–1438.

Van Mooy, B. A. S., and others. 2009. Phytoplankton in the ocean use non-phosphorus lipids in response to phosphorus scarcity. Nature **485:** 69–72.

Vaulot, D., D. Marie, R. J. Olson, and S. W. Chisholm. 1995. Growth of *Prochlorococcus*, a photosynthetic prokaryote, in the equatorial Pacific. Science **286:** 1480–1482.

Walters, R. G., and P. Horton. 1991. Resolution of components of non-photochemical chlorophyll fluorescence quenching in barley leaves. Photosynth. Res. **27:** 121–133.

Waring, J., M. Klenell, U. Bechtold, G. J. C. Underwood, and N. R. Baker. 2010. Light-induced response of oxygen photoreduction, reactive oxygen species production and scavenging in two diatoms species. J. Phycol. **46:** 1206–1217.

Worden, A. Z., J. K. Nolan, and B. Palenik. 2004. Assessing the dynamics and ecology of marine picophytoplankton: The importance of the eukaryotic component. Limnol. Oceanogr. **49:** 168–179.

Wu, J., W. Sunda, E. A. Boyle, and D. M. Karl. 2000. Phosphate depletion in the western North Atlantic Ocean. Science **289:** 759–762.

Associate editor: Robert R. Bidigare

Received: 08 February 2013
Accepted: 03 June 2013
Amended: 04 June 2013